

Energy-Efficient Massive IoT Shared Spectrum Access over UAV-enabled Cellular Networks

Ghaith Hattab, *Student Member, IEEE*, Danijela Cabric, *Senior Member, IEEE*

Abstract

Providing connectivity to a massive number of sensors and machines, commonly known as massive Internet-of-things (IoT), has become a critical use case for fifth-generation new radio (5G-NR). Nevertheless, existing transmission protocols, e.g., orthogonal allocation or spectrum sharing, can be detrimental for cellular users (UEs) and IoT devices due to increased congestion and interference or resource splitting. To this end, we consider to equip cellular networks with unmanned aerial vehicles (UAVs), e.g., drones, acting as mobile data aggregators. Specifically, we propose a transmission protocol for shared spectrum access between IoT devices and UEs, where IoT traffic is collected by drones and then aggregated to the cellular network. Using stochastic geometry, we analyze the performance of the proposed protocol and compare it with existing ones. In addition, we present a stochastic optimization framework that optimizes the transmit power of IoT devices to maximize the average energy-efficiency (EE) of a typical IoT device subject to interference constraints on UEs. Simulation results are presented to validate the effectiveness of the proposed transmission protocol and power control, showing significant improvements of the EE of IoT devices with minimal degradation on the UE spectral efficiency when compared to existing transmission schemes.

Index Terms

5G-NR, cellular networks, Internet-of-things, massive IoT, spectrum sharing, stochastic geometry, UAVs.

I. INTRODUCTION

Fifth-generation new-radio (5G-NR) is set to unlock new application scenarios at different fronts. One specific use case is the native support of a massive number of sensors and machines, collectively known as massive cellular Internet-of-things (IoT) or massive machine-type communications (mMTC) [2]. Indeed, it is envisaged that billions of IoT devices will require Internet-connectivity by 2020, creating transformative economic potentials for operators and

This paper was presented in part at the IEEE Int. Conf. on Wireless and Mobile Computing (WiMoB), Rome, Italy, Oct. 2017 [1]. G. Hattab and D. Cabric are with the Department of Electrical Engineering, University of California, Los Angeles, CA 90095-1594 USA (email: ghattab@ucla.edu, danijela@ee.ucla.edu).

stakeholders, reaching trillions of dollars [3]. Further, the massive IoT market is expected to span many vertical sectors, including smart cities, public safety, and agriculture [4].

The support of IoT services over cellular networks is not new. For instance, recent LTE-A cellular standards, e.g., Rel. 13 and Rel. 14, have introduced new user categories tailored for IoT applications, e.g., CAT-0, CAT-M, and NB-IoT, in addition to enabling extended discontinuous reception (eDRX) to reduce power consumption [5]–[7]. Such IoT optimizations, however, are suitable for services that do not require a large deployment of sensors and machines. Indeed, as the density of IoT devices increases, several challenges emerge [8], [9]. First, collisions among IoT devices increase due to the increased number of access requests, making retransmissions more frequent, and thus affecting their energy-efficiency (EE). Second, interference increases when IoT devices share the same spectrum with cellular users (UE), degrading the coverage needed for the former and reducing the spectral efficiency (SE) for the latter. For these reasons, our objective is to propose a cellular architecture that enables a harmonious coexistence of massive IoT with existing UEs.

A. Related work

The techniques toward the coexistence of IoT devices and UEs can be broadly classified into two categories: orthogonal-based and sharing-based solutions [6], [9]. In the former, resource blocks are split among IoT devices and UEs either over time [10] or frequency [11], [12] as means to avoid interference and congestion. However, resource partitioning inevitably leads to a spectral efficiency tradeoff between IoT devices and UEs. In contrast, in spectrum sharing, all resource blocks are shared between UEs and IoT devices. To control congestion, several techniques have emerged such as access class barring (ACB) [13]–[15], randomized back-off schemes [16], and group paging [17]. These methods, nevertheless, do not address the co-channel interference after access requests are granted. Other techniques include non-orthogonal multiple-access (NOMA) [18] that relies on successive interference cancellation, yet such access technique still has several practical challenges, particularly in multi-cell networks [19]. In this work, we consider complementing the cellular network with unmanned aerial vehicles (UAVs) or drones, acting as a middle layer between IoT devices and base stations (BSs) and enabling a shared spectrum access. We further optimize the transmit power of IoT devices to protect UEs from the co-channel interference.

Data aggregation helps alleviate congestion, and it has emerged as an effective solution to handle massive IoT traffic. An experimental study is discussed in [20] to analyze the impact of IoT data aggregation on cellular networks. In [21]–[24], stochastic geometry is used to analyze the coverage performance and/or the energy consumption using single and/or multiple aggregators. These works, however, consider fixed terrestrial aggregators and focus only on the performance of IoT devices, i.e., the coexistence of IoT devices and UEs is not considered. In this paper, we propose to use mobile aggregators, e.g., drones, that stop at optimized predetermined locations, and we consider shared spectrum access between UEs and massive IoT, where the impact of IoT interference on UEs is analyzed. Using drones as data aggregators has been more recently considered in [25], [26]. For instance, the authors in [25] focus on optimizing the throughput of a single link between a source and a destination, assisted by a relaying UAV, whereas in our work we consider a cellular network and focus on optimizing the EE. In [26], the locations and associations of the drones are optimized to minimize the transmit powers of IoT devices, but the coexistence with UEs is not considered, i.e., the network only includes drones and IoT devices. Finally, implementation and practical considerations for UAV-based IoT platforms are studied in [27], [28].

B. Contributions

A summary of the main contributions is given as follows.

- *Shared-based transmission protocol:* We propose a time-division duplexing (TDD) transmission protocol that provides a shared-spectrum access between massive IoT and UEs over the cellular network in the presence of UAVs that act as data aggregators. We use stochastic geometry [29] to characterize the average available resources for UEs and IoT devices and compare the proposed protocol with a sharing-based protocol via ACB as well as resource splitting via frequency partitioning. We also analyze the coverage performance of the UEs in the presence of IoT devices transmitting to their associated drones.
- *Energy-efficiency maximization:* We present a stochastic optimization framework that aims to optimize the transmit power of the IoT device to maximize its average EE subject to a protection criterion to its nearest UEs. For tractable analysis, the framework is given for a single-cell single-drone (SC-SD) scenario, where we derive the average EE in closed form. We further analyze the interference-to-signal ratio (ISR) at the UE in the same cell with IoT devices, and use its distribution as a protection constraint. Convexity analysis is

presented and the solution of the framework is discussed. Further, we discuss extensions of this framework, including the impact of coordinating the transmit powers of BSs and IoT devices and the case of the single-cell multi-drone (SC-MD) scenario.

We validate the theoretical expression of the EE and the optimization framework for the SC-SD and SC-MD scenarios via Monte Carlo simulations, showing that both frameworks provide significant EE improvements to IoT devices compared to transmitting at the maximum power, which is typically done to extend coverage [5]. We then compare the performance of the proposed protocol with existing ones in a large network. Simulations show that the EE is significantly improved for practical drone altitudes, with minimal degradation to the UE's spectral efficiency in the UL and the DL.

C. Paper organization

The rest of the paper is organized as follows. The system model, the proposed UAV-enabled cellular network, and the key performance metrics, are presented in Section II. A comparison of the proposed transmission protocol and existing ones is presented in Section III. The EE SC-SD maximization framework and its extensions are given in Section IV and Section V, respectively. Simulation results and the main conclusions are given in Section VI and Section VII, respectively.

II. SYSTEM MODEL AND PROPOSED ARCHITECTURE

A. Cellular network model

1) *BSs and UEs*: We consider a stochastic network topology, where we model the locations of BSs using the homogeneous Poisson Point process (HPPP) Φ_B with density λ_B [24]. Each BS is equipped with a multi-antenna array of size M_B , and can multiplex U_B users in a single time-frequency resource block. During downlink (DL) data communications, the BS transmits at a fixed power of P_B , such that each multiplexed user is equally allocated a power of P_B/U_B . For UEs, we assume that they are generated from an independent HPPP Φ_U with density λ_U , where each one is equipped with a single-antenna system and connects to the nearest BS. During uplink (UL) data communications, the UE transmits at a fixed power of P_U .

2) *Ground-to-ground channel model*: For ground-to-ground links, e.g., BS-UE links, we assume a power-law path loss model with a loss of L_0 at a reference distance of 1m and a decaying exponent of α_G . For small-scale fading, we assume a Rayleigh fading channel, with gamma distributed channel power gains, as they model a variety of multi-antenna transmission

modes [30]. Specifically, the channel power gains between the UE and the tagged BS and the UE and an interfering BS are, respectively, modeled as $g_B \sim \Gamma(\Delta_B, 1)$ and $f_B \sim \Gamma(\Psi_B, 1)$. For instance, if the BS uses multi-user zero-forcing transmit beamforming, then the DL desired and interfering channel gains have shapes $\Delta_B = M_B - U_B + 1$ and $\Psi_B = U_B$, respectively [30].

We remark that we focus on a single-tier network for easier exposition in the subsequent analysis. However, it is straightforward to extend this work to multi-tier heterogeneous networks as we have done in our prior work in [1].

B. IoT devices model

Besides providing connectivity to UEs, the cellular network must also provide connectivity for a large number of IoT devices, which are assumed to operate mainly in the UL [4]. Furthermore, we assume that IoT devices are clustered either inherently, e.g., deploying sensors in hotspots to monitor the same physical phenomenon [24], or via a clustering algorithm, as done in [26]. To this end, we model the locations of IoT devices using an independent clustered HPPP process. In particular and similar to [24], we consider the Matern cluster process, where the locations of cluster centers, i.e., parent points, is modeled by the independent HPPP Φ_{Cl} with density λ_{Cl} . In each cluster, IoT devices represent the daughter points of the clustered process, denoted by Φ_M , and they are uniformly distributed in a disk of radius R and with density λ_M . Thus, the average density of IoT devices in the network is $\lambda_M \lambda_{Cl}$. Finally, we assume all IoT devices are single-antenna transmitters, and they transmit at a fixed power of P_M .

Applications where such IoT models are reasonable include the mass deployment of IoT devices across a city, where sensors can be anchored on bridges for infrastructure monitoring, on buildings for utility metering, or in a farm for water management and pest control [4]. Such applications are delay tolerant, yet they require reliable coverage and very long lifetime.

C. Proposed UAV-enabled cellular architecture

We propose to deploy UAVs, e.g., drones, as a middle layer between IoT devices and the cellular infrastructure. The drone acts as a *mobile data aggregator* that is sent by a BS to provide coverage for a cluster of IoT devices. We assume the density of drones, λ_D , is equal to the density of clusters, i.e., $\lambda_D = \lambda_{Cl}$, and each one flies at an altitude of h_D . Further, the drone is equipped with an omni-directional single-antenna cellular transceiver. We discuss the case of a multi-tier drone network, where each tier is defined by a different altitude, in Section V.

1) *Initial access phase:* Since we focus on massive IoT applications with machines and sensors anchored to fixed locations, it is reasonable to assume that the locations of the IoT devices in the cluster are registered in a server or a database, and hence they are known to the mobile operator [4], [26]. In particular, the drone, which is sent by the BS, moves to predetermined *stop points* for UL data aggregation. In this work and for tractable analysis, the stop point of the l -th drone, $(x_{D,l}, y_{D,l}, h_D)$, is the centroid of its cluster of IoT devices. We note that such location minimizes the distance to the typical IoT device, i.e., it can be shown that $(x_{D,l}, y_{D,l}) = \operatorname{argmin}_{(x,y)} \mathbb{E}_{\Phi_M}[d_{M,l}]$, where $d_{M,l}$ is the 3D distance between a typical IoT device and the drone. Finally, we note that the optimization of drone's trajectory, e.g., to maximize lifetime, is outside the scope of this work.

2) *Ground-to-air channel model:* We consider the following popular ground-to-air path loss model for the link between an IoT device and the l -th MDA [26], [31], [32]

$$l_{M \rightarrow D}(d_{M,l}) = \mathbb{P}_{\text{LOS}}(d_{M,l}, h_D) L_0 d_{M,l}^{-\alpha_A} + (1 - \mathbb{P}_{\text{LOS}}(d_{M,l}, h_D)) L_{\text{NLOS}} L_0 d_{M,l}^{-\alpha_A}, \quad (1)$$

where $\mathbb{P}_{\text{LOS}}(d_{M,l}, h_D)$ is the line-of-sight (LOS) probability, L_{NLOS} is the excessive path loss due to non-LOS, and α_A is the ground-to-air path loss exponent. Note that, as investigated in [32], the impact of multi-path fading is negligible in such links and thus it is ignored. The LOS probability is found using the 3GPP UMa-AV channel model, and it can be expressed as [33]

$$\mathbb{P}_{\text{LOS}}(d_{M,l}, h_D) = \min \left\{ \frac{\xi_1}{r_{M,l}}, 1 \right\} (1 - e^{-r_{M,l}/\xi_2}) + e^{-r_{M,l}/\xi_2}, \quad (2)$$

where $r_{M,l} = \sqrt{d_{M,l}^2 - h_D^2}$, and ξ_1 and ξ_2 are some constants as given in [33, Table B-1]. For the link between the BS and the drone, we consider a similar model, which is expressed as

$$l_{B \rightarrow D}(d_{B,l}) = L_{\text{STR}} \cdot (\mathbb{P}_{\text{LOS}}(d_{B,l}, h_D) L_0 d_{B,l}^{-\alpha_A} + (1 - \mathbb{P}_{\text{LOS}}(d_{B,l}, h_D)) L_{\text{NLOS}} L_0 d_{B,l}^{-\alpha_A}), \quad (3)$$

where the attenuation L_{STR} is due to the fact that the BS's antenna array steering direction either points horizontally or is tilted downwards [34]. Such attenuation depends on the drone's relative location with the array's boresight. However, we assume it to be constant for tractable analysis, which is reasonable when the drone is flying at heights higher than the BS's antenna height.

The UAV-enabled cellular network is shown in Fig. 1a, where a drone is sent by a BS to a cluster of IoT devices, stops at $(x_{D,l}, y_{D,l})$ to collect data from IoT devices, and then aggregates the traffic to the BS. An illustration of one realization of the network is also shown in Fig. 1b.

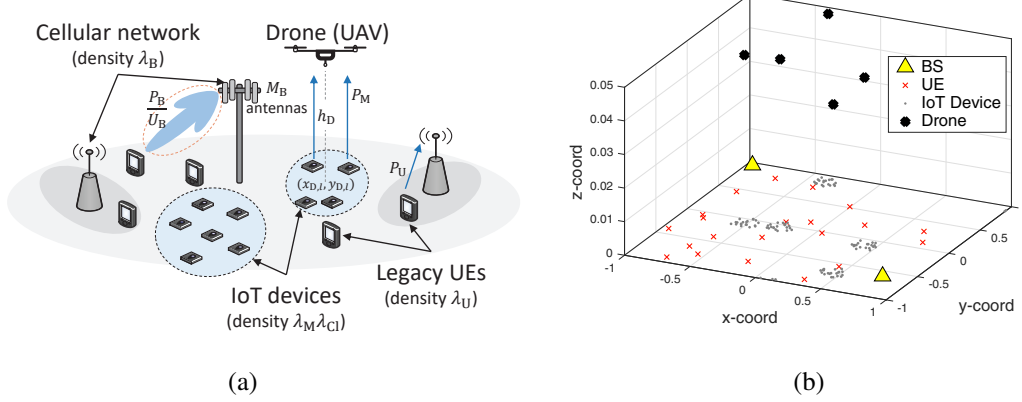


Fig. 1: (a) The proposed UAV-enabled cellular architecture; (b) A spatial realization of the network topology ($\lambda_U = 5\lambda_B$, $\lambda_D = \lambda_B$, and $\lambda_M = 20/\text{cluster}$).

D. Performance Metrics

We consider two key performance metrics: the spectral efficiency (SE) of a typical UE in the UL and DL and the energy efficiency (EE) of a typical IoT device, which are defined next.

1) *UE Spectral Efficiency*: We consider the UE to employ a multi-modulation and coding scheme, and thus the spectral efficiency of a typical UE in the DL/UL is defined as [35]

$$C_{U,\xi} = \bar{\beta}_{U,\xi} \sum_{k=1}^{K_U} \log_2(1 + \tau_{U,k}) \mathbf{1}(\tau_{U,k+1} \geq \gamma_{U,\xi} \geq \tau_{U,k}), \quad (4)$$

where $\xi \in \{\text{DL}, \text{UL}\}$, $\gamma_{U,\xi}$ is the signal-to-interference-plus-noise ratio (SINR), $\{\tau_{U,k}\}$ are the SINR thresholds, $\mathbf{1}(\cdot)$ is the indicator function, and $\bar{\beta}_{U,\xi}$ is a pre-log term that denotes the UE long-term available resources in time, frequency, and space. This rate model assumes K_U possible thresholds, and it is a generalization of the single-rate model, i.e., $K_U = 1$, that is commonly used in the literature [30], [36]. We remark that in this work, we use the mean load approximation to analytically characterize the BS load, i.e., we assume that the load $\bar{\beta}_{U,\xi}$ is independent of $\gamma_{U,\xi}$ [35], [36].

2) *IoT Energy Efficiency*: Since the majority of IoT devices are battery-powered, the EE of the transmission protocol is critical, which is defined as the ratio of the achieved rate to the total power consumption. More formally, the EE of a typical IoT device is defined as [37]

$$E_M = \frac{\bar{\beta}_M \sum_{k=1}^{K_M} \log_2(1 + \tau_{M,k}) \mathbf{1}(\tau_{M,k+1} \geq \gamma_M \geq \tau_{M,k})}{P_{CP} + \eta^{-1} P_M}, \quad (5)$$

where P_{CP} is a constant that quantifies the circuit power consumption, η is the power amplifier efficiency, and $\bar{\beta}_M$ and γ_M are the IoT device long-term resources and SINR, respectively. Finally,

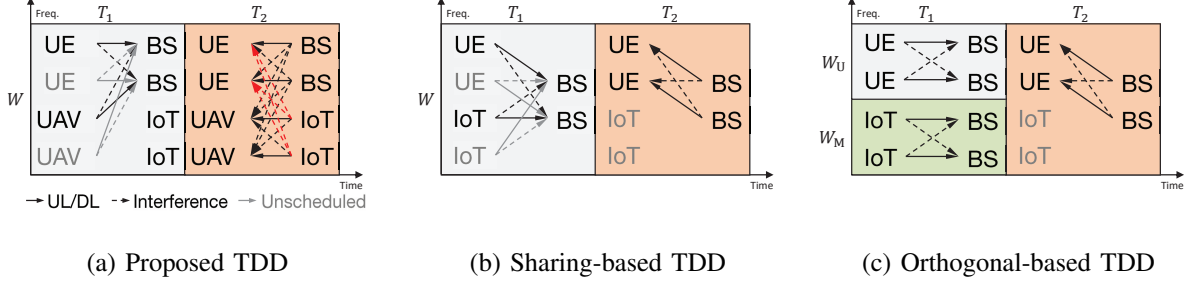


Fig. 2: Comparison of the different TDD transmission protocols.

we note that (5) inherently considers the coverage performance since a zero rate, and hence zero EE, is achieved if $\gamma_M < \tau_{M,1}$.

III. PROPOSED TRANSMISSION PROTOCOL

In this section, we present the proposed transmission protocol to enable shared spectrum access between massive IoT and UEs over UAV-enabled cellular networks. We then analyze the average allocated resources of the UE and the IoT device under the proposed protocol and compare it to those achieved under existing transmission protocols.

We focus on TDD cellular networks, and thus the proposed protocol is divided into two slots: T_1 and T_2 . In the first time slot, the UE operates in the UL, communicating with its tagged BS. Similarly, in this slot, we treat the drone as another UE, which aggregates previously collected data from IoT devices and sends it to its tagged BS. In the second time slot, the UE operates in the DL, whereas the IoT device operates in the UL, communicating with its associated drone, as shown in Fig. 2a. The proposed protocol is motivated as follows.

- **Maximum bandwidth:** The protocol allows the IoT device to share the same time-frequency block with the UE, i.e., no resource splitting is used.
- **Reducing congestion:** When the UE operates in the UL, it competes for scheduling with drones instead of IoT devices, and thus the channel congestion is significantly reduced.
- **Limiting the impact of IoT interference:** The shared access paradigm inevitably leads to additional interference from IoT devices into UEs. However, when IoT devices transmit data in the UL, UEs operate in the DL, where their tagged BSs transmit at much higher power than the transmit power of IoT devices as $P_B \gg P_M$.

A. Characterization of average resources in the proposed and existing protocols

For tractable analysis, we assume that a proportional fair scheduler is used, e.g., round-robin, and thus under the mean load approximation [36], the average load is inversely proportional to the average number of devices connected to the same source.

1) *Proposed protocol:* Let $\bar{\beta}_{U,UL}^P$ denote the average allocated resources to a typical UE operating in the UL under the proposed protocol. Then, it can be shown that

$$\begin{aligned}\bar{\beta}_{U,UL}^P &\stackrel{(a)}{=} \underbrace{W}_{\text{Freq.}} \times \underbrace{U_B}_{\text{Space}} \times \underbrace{T_1 \left(\frac{1}{N_{B,UL}^P} \right)}_{\text{Time}} \\ &\stackrel{(b)}{=} W \times U_B \times T_1 \left(\frac{\lambda_B}{\lambda_U + \lambda_D} \right),\end{aligned}\tag{6}$$

where (a) follows since the entire bandwidth W is allocated to the UE, U_B UEs can be spatially multiplexed by the same BS, and the portion of the time allocated to the UE is inversely proportional to the average number of devices connected to the BS, i.e., $N_{B,UL}^P$. Here, (b) follows by showing that the average number of UEs (or drones) connected to the BS under the nearest BS association is λ_U/λ_B (or λ_D/λ_B) [36]. Similarly, the average resources of the UE in the DL is expressed as $\bar{\beta}_{U,DL}^P = W \times U_B \times T_2 \left(\frac{\lambda_B}{\lambda_U} \right)$, which follows since in the second time slot, no IoT devices are connected to the BS under the proposed protocol. For the IoT device, it can be shown that the average resources is given as $\bar{\beta}_M^P = W \times T_2 \lambda_M^{-1}$, which follows since the average number of IoT devices per cluster is λ_M , and the drone multiplexes one IoT device per time-frequency slot. Note that for low-rate applications, the drone can divide the bandwidth W into smaller frequency blocks and serve multiple IoT devices, one per frequency block. This does not change $\bar{\beta}_M^P$ since the decrease in frequency resources is equally compensated by increased time resources.

2) *Comparison with sharing-based protocol:* In the sharing-based protocol, the IoT device is registered as another UE, as shown in Fig. 2b. To control channel congestion, the 3GPP standard proposes one mechanism, namely *access class barring* (ACB), which prioritizes UE traffic over IoT devices [9]. More formally, each BS broadcasts a parameter $0 \leq \kappa \leq 1$ to all IoT devices in vicinity. The IoT device then generates a random number $n \in [0, 1]$ before initiating a channel access request. If $n > \kappa$, then the IoT device does not request access. Clearly, for $\kappa = 1$, the protocol simplifies to a standard sharing protocol that is agnostic to the device type. Let $\bar{\beta}_{U,UL}^S$ denote the average allocated resources to a typical UE operating in the UL under

the sharing-based protocol. Then, we have $\bar{\beta}_{U,UL}^S = W \times U_B \times T_1 \left(\frac{\lambda_B}{\lambda_U + \kappa \lambda_M \lambda_{Cl}} \right)$, which follows since the average number of IoT devices per BS is $\lambda_M \lambda_{Cl} / \lambda_B$, yet only a fraction, κ , of them request access. Clearly, for $\bar{\beta}_{U,UL}^S > \bar{\beta}_{U,UL}^P$, we must have $\kappa < \lambda_M$, yet this degrades the average resources allocated to the IoT device. Indeed, the average allocated resource of a typical IoT device under the sharing protocol is given as

$$\begin{aligned} \bar{\beta}_M^S &= \mathbb{P}(n > \kappa) \bar{\beta}_{M|n>\kappa}^S + \mathbb{P}(n \leq \kappa) \bar{\beta}_{M|n \leq \kappa}^S \\ &= W \times U_B \times \kappa T_1 \left(\frac{\lambda_B}{\lambda_U + \kappa \lambda_M \lambda_{Cl}} \right) \\ &\stackrel{(a)}{\leq} \bar{\beta}_M^P \left(\frac{U_B \lambda_B}{\lambda_U + \lambda_{Cl}} \right) \end{aligned} \quad (7)$$

where (a) follows using $\kappa < \lambda_M$ and assuming $T_1 = T_2$. Since the density of UEs is typically higher than the density of BSs, i.e., $\lambda_U \gg U_B \lambda_B$, we get $\bar{\beta}_M^S < \bar{\beta}_M^P$. Finally, for the second time slot, we have $\bar{\beta}_{U,DL}^S = \bar{\beta}_{U,DL}^P$ for the UE.

3) *Comparison with orthogonal-based protocol:* Alternative to using ACB to resolve channel congestion, 3GPP has also proposed the separation of frequency resources [9], as shown in Fig. 2c. Let $W_U \in [0, W]$ be the portion of spectrum allocated for UEs, then the average allocated resources for a typical UE in the UL under this protocol is $\bar{\beta}_{U,UL}^O = W_U \times U_B \times T_1 \left(\frac{\lambda_B}{\lambda_U} \right)$. If $W_U/W > \lambda_U/(\lambda_U + \lambda_D)$, then we have $\bar{\beta}_{U,UL}^O > \bar{\beta}_{U,UL}^P$. However, this comes at the expense of reducing the resources allocated to the IoT device since we have

$$\begin{aligned} \bar{\beta}_M^O &= W_M \times U_B \times T_1 \left(\frac{\lambda_B}{\lambda_M \lambda_{Cl}} \right) \\ &\stackrel{(a)}{<} W \times U_B \times \frac{T_1}{\lambda_M} \left(\frac{\lambda_B}{\lambda_U + \lambda_{Cl}} \right) \\ &\stackrel{(b)}{<} \bar{\beta}_M^P, \end{aligned} \quad (8)$$

where (a) follows from the fact that $W_M = W - W_U$ and thus $\frac{W_U}{W} > \frac{\lambda_U}{\lambda_U + \lambda_{Cl}} \iff \frac{W_M}{W} < \frac{\lambda_{Cl}}{\lambda_U + \lambda_{Cl}}$. In addition, (b) follows assuming $T_1 = T_2$ and the density of UEs is high. Finally and similar to the sharing-based protocol, we have $\bar{\beta}_{U,DL}^O = \bar{\beta}_{U,DL}^P$ for the UE.

To summarize, for the sharing protocol to outperform the proposed one in terms of resource allocation for the UE, we must use aggressive ACB with very small values of κ , which inevitably affects the IoT EE as the average allocated resources is decreased. For the orthogonal allocation to outperform the proposed protocol in terms of the UE performance, nearly all resources should be allocated to the UE, i.e., $W_U \rightarrow W$, since $\lambda_U \gg \lambda_D$, and this also limits the resources allocated to the IoT device.

B. Analysis of IoT Interference on UEs

While the proposed protocol improves the average allocated resources of a typical UE, in comparison with sharing-based and orthogonal-based protocols, the signal-to-interference ratio (SIR) of a typical UE degrades due to the presence of an additional interference term generated from IoT devices (cf. Fig. 2a). Specifically, the SIR of a typical UE can be written as

$$\tilde{\gamma}_{\text{U,DL}}^{\text{P}} = \frac{\frac{P_{\text{B}}}{U_{\text{B}}} g_{\text{B}} L_0 x_{\text{B}}^{-\alpha_{\text{G}}}}{\sum_{y_b \in \Phi'_{\text{B}}} \frac{P_{\text{B}}}{U_{\text{B}}} f_b L_0 y_b^{-\alpha_{\text{G}}} + \sum_{z_m \in \Phi'_{\text{M}}} P_{\text{M}} f_m L_0 z_m^{-\alpha_{\text{G}}}}, \quad (9)$$

where Φ'_{B} is the set of interfering BSs, Φ'_{M} is the set of interfering IoT devices, $f_m \sim \Gamma(1, 1)$, x_{B} is the distance to the tagged BS, y_b is the distance to the b -th interfering BS, and z_m is the distance to the m -th interfering IoT device. Next, we derive the coverage probability of the UE under the proposed protocol to highlight the key parameters that affect the UE's coverage.

The coverage probability is defined as $\mathbb{C}_{\text{U,DL}}^{\text{P}}(\tau) \triangleq \mathbb{P}(\tilde{\gamma}_{\text{U,DL}}^{\text{P}} \geq \tau)$, which can be rewritten as

$$\mathbb{C}_{\text{U,DL}}^{\text{P}}(\tau) \stackrel{(a)}{=} 2\pi\lambda_{\text{B}} \int_0^\infty x \mathbb{E}_{g_{\text{B}}} \left[F_{I_{\text{U}}} \left(\frac{g_{\text{B}}}{\tau x^{\alpha_{\text{G}}}} \right) \right] e^{-\pi\lambda_{\text{B}}x^2} dx, \quad (10)$$

where (a) follows from the distribution of the distance from the UE to the tagged BS [36], and $F_{I_{\text{U}}}(\cdot)$ is the cumulative distribution function (CDF) of the interference. Using the Gil-Pelaez Inversion theorem [38] to compute the interference CDF, we get the following theorem.

Theorem 1. *The coverage probability of the UE under the proposed protocol is expressed as*

$$\mathbb{C}_{\text{U,DL}}^{\text{P}}(\tau) = \frac{1}{2} - \frac{\Upsilon(\tau, \lambda_{\text{B}}, \lambda_{\text{D}}, \hat{P}_{\text{B,M}})}{\pi}, \quad (11)$$

where $\hat{P}_{\text{B,M}} = \text{sinc}^{-1}(\delta_{\text{G}})P_{\text{M}}U_{\text{B}}/P_{\text{B}}$, $\delta_{\text{G}} = 2/\alpha_{\text{G}}$, and

$$\Upsilon(\tau, \lambda_{\text{B}}, \lambda_{\text{D}}, \hat{P}_{\text{B,M}}) = \int_0^\infty \frac{1}{t} \text{Im} \left\{ \frac{(1 + jt/\tau)^{-\Delta_{\text{B}}}}{{}_2F_1(\delta_{\text{G}}, \Psi_{\text{B}}; 1 - \delta_{\text{G}}; jt) + \frac{\lambda_{\text{D}}}{\lambda_{\text{B}}} \hat{P}_{\text{B,M}}^{\delta_{\text{G}}} (-jt)^{\delta_{\text{G}}}} \right\} dt. \quad (12)$$

Proof: See Appendix A. ■

The expression is given in a single integral form that can be efficiently evaluated using a numerical software. The key insight here is that the degradation of the UE coverage due to the presence of IoT devices depends mainly on two factors: (i) the ratio of the transmit power of the IoT device to the power allocated to the UE, i.e., $P_{\text{M}}/(P_{\text{B}}/U_{\text{B}})$ and (ii) the average number of drones per BS, i.e., $\lambda_{\text{D}}/\lambda_{\text{B}}$. To see this, note that the coverage probability in the absence of IoT devices is $\mathbb{C}_{\text{U,DL}}^{\text{N}}(\tau) = \frac{1}{2} - \frac{1}{\pi} \int_0^\infty \frac{1}{t} \text{Im} \left\{ \frac{(1 + jt/\tau)^{-\Delta_{\text{B}}}}{{}_2F_1(\delta_{\text{G}}, \Psi_{\text{B}}; 1 - \delta_{\text{G}}; jt)} \right\} dt$, and thus using stochastic dominance, i.e., $\mathbb{C}_{\text{U,DL}}^{\text{N}}(\tau) \geq \mathbb{C}_{\text{U,DL}}^{\text{P}}(\tau)$, we have

$$\int_0^\infty \frac{1}{t} \text{Im} \left\{ \frac{(1 + jt/\tau)^{-\Delta_{\text{B}}}}{{}_2F_1(\delta_{\text{G}}, \Psi_{\text{B}}; 1 - \delta_{\text{G}}; jt)} \right\} dt \leq \Upsilon(\tau, \lambda_{\text{B}}, \lambda_{\text{D}}, \hat{P}_{\text{B,M}}), \quad (13)$$

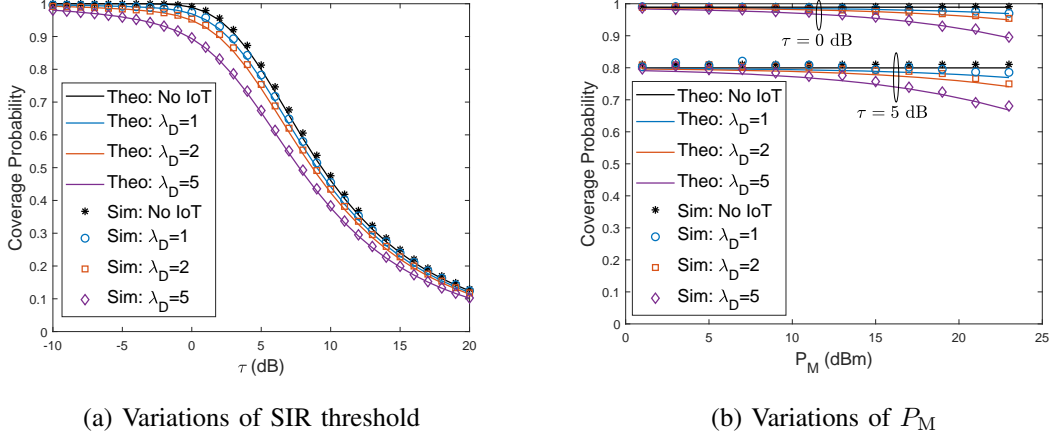


Fig. 3: The UE DL coverage performance with and without IoT devices.

where the gap above decreases as $\lambda_D/\lambda_B \rightarrow 0$ and/or $P_M/(P_B/U_B) \rightarrow 0$.

We validate the theoretical expression with Monte Carlo simulations, using the same parameters in Table I. Fig. 3a shows the distribution of coverage in the presence and absence of IoT devices. It is observed that increasing the number of drones decreases the coverage, yet the degradation is not severe, e.g., the median SIR merely degrades by 1.7dB under the proposed protocol with $\lambda_D/\lambda_B = 5$. Recall that here a drone is assigned to a single cluster. However, if a single drone is assigned instead to serve multiple clusters, moving from one stop point to another, then the interference on UEs from IoT transmission decreases, e.g., median SIR degradation is less than 0.36dB when $\lambda_D/\lambda_B = 1$. Nevertheless, the cost of reducing this interference is the increased delay on IoT devices, leading eventually to degradation of the IoT energy efficiency when $\lambda_M \lambda_{CI} \gg 1$. To this end, another approach to limit the interference is to reduce the IoT transmit power, as shown in Fig. 3b. In the next section, we focus on optimizing the IoT transmit power such that the IoT EE is maximized and the IoT interference is controlled.

IV. IOT ENERGY-EFFICIENCY MAXIMIZATION

In this section, we present a stochastic optimization framework that maximizes the average EE of an IoT device under the proposed protocol. The framework takes the following form

$$\begin{aligned}
 & \underset{P_M}{\text{maximize}} && \mathbb{E}[E_M] \\
 & \text{subject to} && f(I_U) \leq \epsilon, \\
 & && P_M \in \mathcal{P},
 \end{aligned} \tag{14}$$

where the $f(\cdot)$ is an interference constraint to protect UEs and \mathcal{P} is the feasible set of transmit powers. Note that this is a stochastic optimization framework, as the objective function is the mean of a random variable, and the expectation is taken with respect to spatial realizations. Note further that such formulation aims to optimize a single variable P_M , significantly reducing the complexity of implementation, i.e., the drone merely solves the problem off-line and then broadcasts the optimal transmit power, over a control channel, to all of its IoT devices.

There are two challenges to solve (14). The first one is that the objective function is intractable due to the ground-to-air channel model from interfering BSs and IoT devices into drones. The second one is that the UE coverage probability in (11) is given in an integral form, making it not amenable to use as a UE protection criterion. For these reasons, we focus on optimizing the EE in a single-cell single-drone (SC-SD) setting, i.e., we ignore the interference from BSs and IoT devices outside the cell of the typical IoT device. Such framework is shown to be tractable, which helps glean useful insights. We will further evaluate the solution of the SC-SD framework in the large network case, i.e., many drones and many cells, via Monte Carlo simulations.

A. Average IoT EE in the SC-SD Case

Let \hat{E}_M and $\hat{\gamma}_M$ denote the IoT EE and IoT UL SINR in the SC-SD case, respectively, and let $p = P_M$ for notational simplicity. Then, the average EE under the proposed protocol, i.e., $\bar{E}_M(p) \triangleq \mathbb{E}[\hat{E}_M]$, can be written as

$$\begin{aligned} \bar{E}_M(p) &= \frac{\bar{\beta}_M^P \sum_{k=1}^{K_M} \log_2(1 + \tau_{M,k}) \mathbb{E}[\mathbf{1}(\tau_{M,k+1} \geq \hat{\gamma}_M(p) \geq \tau_{M,k})]}{P_{CP} + \eta^{-1}p}, \\ &= \frac{\bar{\beta}_M^P \sum_{k=1}^{K_M} \mu_k \mathbb{P}(\hat{\gamma}_M(p) \geq \tau_{M,k})}{P_{CP} + \eta^{-1}p}, \end{aligned} \quad (15)$$

where $\mu_1 = \log_2(1 + \tau_{M,1})$ and $\mu_k = \log_2(1 + \tau_{M,k+1}) - \log_2(1 + \tau_{M,k})$ for $k > 1$.

In a single cell, the drone receives signals from IoT devices in its cluster and receives interference from the tagged BS, which operates in the DL. The next proposition presents the distributions of the received desired signal and interference powers at the drone, which will be useful to evaluate $\mathbb{P}(\hat{\gamma}_M(p) \geq \tau_{M,k})$.

Proposition 1. *The distribution of the desired signal power, $S_M = P_M l_{M \rightarrow D}(d_{M,l})$, at a typical drone is expressed as*

$$\mathbb{P}(S_M \leq \tau) = 1 - \frac{(P_M L_M / \tau)^{\delta_A} - h_D^2}{R^2}, \quad (16)$$

where $\delta_A = 2/\alpha_A$, $L_M = L_0((1 - L_{\text{NLOS}})\bar{\mathbb{P}}_{\text{LOS},M} + L_{\text{NLOS}})$, $\bar{\mathbb{P}}_{\text{LOS},M}$ is the average of (2), which is computed numerically, and $\tau \in [P_M L_M (R^2 + h_D^2)^{-1/\delta_A}, P_M L_M h_D^{-\alpha_A}]$. In addition, the distribution of the interference signal power $I_B = P_B l_{B \rightarrow D}(d_{B,l})$ is given as

$$\mathbb{P}(I_B \leq \tau) = \exp(\pi \lambda_B h_D^2) \cdot \exp\left(-\pi \lambda_B (P_B L_B / \tau)^{\delta_A}\right), \quad (17)$$

where $L_B = L_0((1 - L_{\text{NLOS}} L_{\text{STR}})\bar{\mathbb{P}}_{\text{LOS},B} + L_{\text{NLOS}} L_{\text{STR}})$ and $\tau \in [0, P_B L_B h_D^{-\alpha_A}]$.

Proof: See Appendix B. ■

Remark: It is observed from (16) that as h_D increases, the variations in S_M reduces since $\tau \in [P_M L_M (R^2 + h_D^2)^{-1/\delta_A}, P_M L_M h_D^{-\alpha_A}]$, i.e., the distribution of S_M becomes more concentrated around the median. This follows because the drone location is optimized to reduce the average 2D distance to a typical IoT device, increasing the LOS probability particularly when $h_D \geq R$. Similarly, it is observed from (17) that increasing the density of BSs increases the interference as the average distance between the drone and its tagged BS decreases. Furthermore, it can be shown that increasing the drone's height decreases I_B , but not as rapidly as the decrease in S_M .

Using Proposition 1, we derive the coverage probability and the average EE of the IoT device.

Theorem 2. *The coverage probability of an IoT device in the SC-SD case is given as*

$$\mathbb{P}(\hat{\gamma}_M \geq \tau) \approx \exp(\pi \lambda_B h_D^2) \cdot \exp\left(-\pi \lambda_B \left(\frac{\frac{P_M \tilde{L}_M}{\tau} - P_N}{P_B L_B}\right)^{-\delta_A}\right), \quad (18)$$

where $\tilde{L}_M = L_M(\frac{R^2}{2} + h_D^2)^{-1/\delta_A}$ and P_N is the noise power. In addition, the average EE of an IoT device is expressed as

$$\bar{E}_M(p) = \frac{\bar{\beta}_M^P \exp(\pi \lambda_B h_D^2) \sum_{k=1}^{K_M} \mu_k \exp\left(-\frac{\pi \lambda_B}{(P_B L_B)^{-\delta_A}} \left(\frac{p \tilde{L}_M}{\tau_k} - P_N\right)^{-\delta_A}\right)}{P_{\text{CP}} + \eta^{-1} p}. \quad (19)$$

Proof: The coverage probability can be written as

$$\mathbb{P}(\hat{\gamma}_M \geq \tau) \triangleq \mathbb{P}\left(\frac{S_M}{I_B + P_N} \geq \tau\right) \approx \mathbb{P}\left(I_B \leq \frac{\tilde{S}_M}{\tau} - P_N\right), \quad (20)$$

where we have used the median received signal power \tilde{S}_M computed from (16) to approximate the coverage (recall that S_M has small variations particularly when $h_D \geq R$). Thus, using (17), we arrive at (18). ■

B. IoT Interference Constraint

In this section, we propose to use the distribution of the interference-to-signal ratio (ISR) as a protection criterion. We note that in [39], [40], the mean of ISR (MISR) has been used as a metric to compare between different interference mitigation techniques over cellular networks with stochastic topologies. Yet, using the ISR distribution provides more flexibility compared to the MISR, e.g., the protection criterion can be designed to limit the median, the 95th percentile, etc. The ISR is defined as $\text{ISR}_U = \frac{\mathbb{E}_{f_M}[\hat{I}_{U,M}]}{\mathbb{E}_{g_B}[S_B]}$, where $\hat{I}_{U,M}$ is the interference from the typical IoT device to its nearest UE and S_B is the received desired signal power at the UE from its tagged BS. We note, similar to the MISR metric, the expectation is first taken with respect to channel realizations. The distribution is thus given as

$$\begin{aligned}
 \mathbb{P}(\text{ISR}_U \geq \rho) &\stackrel{(a)}{=} \mathbb{P}\left(\frac{P_M z_M^{-\alpha_G}}{\frac{\Delta_B P_B}{U_B} z_B^{-\alpha_G}} \geq \rho\right) \\
 &= \mathbb{P}\left(\frac{z_B}{z_M} \geq \left(\rho \frac{\Delta_B P_B}{U_B P_M}\right)^{1/\alpha_G}\right) \\
 &\stackrel{(b)}{=} \mathbb{E}_{z_M} \left[\exp\left(-\pi \lambda_B z_M^2 \left(\rho \frac{\Delta_B P_B}{U_B P_M}\right)^{\delta_G}\right) \right] \\
 &\stackrel{(c)}{=} \left[1 + \frac{\lambda_B}{\lambda_U} \left(\rho \frac{\Delta_B P_B}{U_B P_M}\right)^{\delta_G} \right]^{-1},
 \end{aligned} \tag{21}$$

where (a) follows from the mean of desired and interference power channel gains, (b) follows using the complementary CDF of the distance from the UE to its tagged BS, and (c) follows by taking the expectation with respect to the distance between the IoT device and the nearest UE.

C. SC-SD Stochastic Optimization Framework

Using (19) as an objective function and the ISR expression in (21) as an interference constraint, i.e., $f(I_U) \leq \epsilon \Leftrightarrow \mathbb{P}(\text{ISR}_U \geq \rho) \leq \epsilon$, we get the following optimization problem

$$\begin{aligned}
 &\underset{P_M}{\text{maximize}} && \frac{\sum_{k=1}^{K_M} \mu_k \exp\left(-\frac{\pi \lambda_B}{(P_B L_B)^{-\delta_A}} \left(\frac{P_M \tilde{L}_M}{\tau_k} - P_N\right)^{-\delta_A}\right)}{P_{\text{CP}} + \eta^{-1} P_M} \\
 &\text{subject to} && P_M \leq \rho \left(\frac{\Delta_B P_B}{U_B}\right) \left(\frac{\lambda_B}{\lambda_U} \cdot \frac{\epsilon}{1-\epsilon}\right)^{1/\delta_G}, \\
 &&& P_M^{\min} \leq P_M \leq P_M^{\max},
 \end{aligned} \tag{22}$$

where P_M^{\min} and P_M^{\max} are the minimum and maximum allowable transmit powers, respectively. In what follows, we denote the numerator of the objective function, i.e., the rate, by $r(P_M)$, and

Algorithm 1 Dinkelbach's algorithm to solve the SC-SD optimization

```

1: procedure ( $\zeta > 0; i = 0; \nu_i = 0$ )
2:   while  $H(\nu_i) > \zeta$  do
3:      $p_i^* = \min \left\{ P_M^{\max}, \rho \left( \frac{\Delta_B P_B}{U_B} \right) \left( \frac{\lambda_B}{\lambda_U} \cdot \frac{\epsilon}{1-\epsilon} \right)^{1/\delta_G}, \mathbf{ROOT}(r'(p) - \eta^{-1}\nu_i) \right\}$ 
4:      $H(\nu_i) = r(p_i^*) - \nu_i c(p_i^*)$  and  $\nu_{i+1} = \frac{r(p_i^*)}{c(p_i^*)}$ 
5:      $i = i + 1$ 
6:   end while
7:   return  $P_M^* = p_i^*$ 
8: end procedure

```

the denominator, i.e., power consumption, by $c(P_M)$. The following proposition shows that the problem in (22) is quasiconcave, and thus a local maximum is a global one [41].

Proposition 2. *The objective function in (22) is quasiconcave and unimodal, whereas the constraints are all affine. Hence, the optimization problem is quasiconcave.*

Proof: The proof follows from showing that $r(p)$ is S-shaped in p (see Appendix C). ■

Since the problem has a single optimizing variable, a line search is sufficient to solve the problem. However, in what follows we discuss a specific algorithm to solve the problem, as its generalization will be used for the SC-MD case in Section V. To solve the optimization problem, we note that if the following condition is satisfied

$$\tau_k \leq \frac{P_M^{\min} \tilde{L}_M}{P_N + P_B L_B \left(\frac{\delta_A \pi \lambda_B}{1 + \delta_A} \right)^{1/\delta_A}} \quad \forall k, \quad (23)$$

then the optimization problem can be transformed from a quasiconcave problem into a concave one using the Charnes-Cooper Transform [41]. Thus, a standard convex optimization solver can be used to solve the problem. When the condition in (23) is not satisfied, i.e., for general thresholds, then the problem can be efficiently solved using the Dinkelbach's algorithm [42], which converges super-linearly to the global optimal solution. The algorithm that specifically solves (22) is summarized in Algorithm 1. In essence, the algorithm seeks to find the root of the auxiliary function $H(\nu) = \max_{p \in \mathcal{P}} \{r(p) - \nu c(p)\}$, which is achieved at the point that maximizes the optimization problem [42]. Finally, a closed-form solution can be derived for the special

case $K_M = 1$ and $\alpha_A = 2$. Specifically, the objective function, in this case, is maximized at

$$p_{\text{unconst}}^* = \frac{\tau_{M,1}(2P_N + \pi\lambda_B P_B L_B) + \sqrt{\pi\tau_{M,1}\lambda_B P_B L_B(4P_N\tau_{M,1} + 4\tilde{L}_M\eta P_{CP} + \pi\tau_{M,1}\lambda_B P_B L_B)}}{2\tilde{L}_M}, \quad (24)$$

and thus the optimal transmit power is $P_M^* = \min\{P_M^{\max}, \rho(\frac{\Delta_B P_B}{U_B}) \left(\frac{\lambda_B}{\lambda_U} \cdot \frac{\epsilon}{1-\epsilon}\right)^{1/\delta_G}, p_{\text{unconst}}^*\}$. It is observed from (24) that the optimal power increases for: (i) higher target threshold $\tau_{M,1}$ to meet the new coverage requirement, (ii) higher BS transmit power P_B or higher BS density λ_B to combat the increased interference from the cellular network, or (iii) higher PA efficiency η to utilize the decrease in power consumption.

V. GENERALIZATIONS TO THE SC-SD FRAMEWORK

In this section, we show how the SC-SD framework can be further generalized to other frameworks, including UAV-BS coordination and the single-cell multi-drone (SC-MD) case.

A. EE Maximization with UAV-BS Coordination

Another critical parameter to the IoT EE performance is the BS transmit power since the objective function and the interference constraint in (22) depend on P_B . To this end, if the optimal transmit power P_M^* satisfies the interference constraint with strict inequality, then the IoT EE can be further improved via UAV-BS coordination. In particular, the BS can transmit, in this case, at lower power so that the constraint is met with equality, reducing the interference seen at the drone. In return, P_M can be set lower due to the reduction in interference, and thus the EE is further improved. This procedure can be done recursively, as summarized in Algorithm 2, until no further improvements are achieved. Here, P_B^{\min} and P_B^{\max} determine the range of the feasible BS transmit power.

B. EE Optimization in heterogeneous single-cell multi-drone case

In this section, we consider the single-cell multi-drone case (SC-MD), where each cell has multiple drones, each serving a cluster of IoT devices. We can further assume each drone belongs to a different tier, i.e., we consider an N -tier drone network such that the l -th tier drone flies at an altitude of $h_{D,l}$ and serves an IoT cluster of radius R_l . The IoT device in a cluster served by the l -th drone transmits at power $P_{M,l}$.

Algorithm 2 Joint UAV-BS transmit power coordination

```

1: procedure ( $P_{B,0} = P_B^{\max}; \zeta > 0$ )
2:   while  $|\bar{E}(P_{M,i+1}) - \bar{E}(P_{M,i})| > \zeta$  do
3:     Update constraint:  $I_{\text{const},i} = \rho \left( \frac{\Delta_B P_{B,i}}{U_B} \right) \left( \frac{\lambda_B}{\lambda_U} \cdot \frac{\epsilon}{1-\epsilon} \right)^{1/\delta_G}$ 
4:     Solve for  $P_{M,i+1}$  in (22) using Algorithm 1
5:     Update BS transmit power:  $P_{B,i+1} = \min \left( \max \left( \frac{P_{M,i+1}}{\rho \frac{\Delta_B}{U_B} \left( \frac{\lambda_B}{\lambda_U} \cdot \frac{\epsilon}{1-\epsilon} \right)^{1/\delta_G}}, P_B^{\min} \right), P_B^{\max} \right)$ 
6:      $i = i + 1$ 
7:   end while
8:   return  $P_M^* = P_{M,i}$  and  $P_B^* = P_{B,i}$ 
9: end procedure

```

The challenge in the multi-drone is that the objective function can no longer be given in a closed-form expression due to the complicated ground-to-air path loss model between multiple interferers and the drone. Here, the interferers, with respect to a given drone, are the tagged BS and the other IoT devices transmitting to their respective drones in the same cell. To this end, we propose to model the different interference sources in the cell as one Poissonian source with a transmit power equal to the sum of transmit powers of all interferers. Such approach ensures a tractable formulation, and will be validated in the simulations section. Under this modeling assumption, the EE of an IoT device served by the l -th drone tier can be written as

$$\bar{E}_l(\mathbf{P}_M) \triangleq \frac{\bar{\beta}_M^P \exp(\pi \lambda_B h_{D,l}^2) \sum_{k=1}^{K_M} \mu_k \exp \left(-\frac{\pi \lambda_B \left(\frac{P_{M,l} \tilde{L}_{M,l}}{\tau_k} - P_N \right)^{-\delta_A}}{(P_B L_B + \sum_{n \neq l} P_{M,n} \tilde{L}_{M,n})^{-\delta_A}} \right)}{P_{CP} + \eta^{-1} P_{M,l}}, \quad (25)$$

where \mathbf{P}_M is the vector of transmit powers. Next, we discuss two common formulations for the EE optimization in the SC-MD case.

1) *Max-min formulation:* In this formulation, the objective is to maximize the minimum EE of a typical IoT device. Such formulation is a conservative one that aims to improve the worst case scenario. In particular, the max-min EE maximization is given as

$$\begin{aligned} & \underset{\mathbf{P}_M}{\text{maximize}} \quad \min_l \quad \bar{E}_l(\mathbf{P}_M) \\ & \text{subject to} \quad \sum_l P_{M,l} \leq \rho \left(\frac{\Delta_B P_B}{U_B} \right) \left(\frac{\lambda_B}{\lambda_U} \cdot \frac{\epsilon}{1-\epsilon} \right)^{1/\delta_G}, \\ & \quad P_M^{\min} \leq P_{M,l} \leq P_M^{\max} \quad \forall l. \end{aligned} \quad (26)$$

The EE expression in (26) is still quasiconcave, and since the objective function is the minimum of quasiconcave functions, it remains quasiconcave. Thus, the max-min framework is

Algorithm 3 Generalized Dinkelbach's algorithm to solve the SC-MD optimization

```

1: procedure ( $\zeta > 0; i = 0; \nu_i = 0$ )
2:   while  $H(\nu) > \zeta$  do
3:      $\mathbf{p}_{M,i}^* = \operatorname{argmax}_{\mathbf{p} \in \hat{\mathcal{P}}} \left\{ \min_l \{r_l(\mathbf{p}) - \nu_i c_l(\mathbf{p})\} \right\}$   $\left[ \mathbf{p}_{M,i}^* = \operatorname{argmax}_{\mathbf{p} \in \hat{\mathcal{P}}} \{ \sum_l r_l(\mathbf{p}) - \nu_{i,l} c_l(\mathbf{p}) \} \right]$ 
4:      $H(\nu_i) = \min_l \{r_l(\mathbf{p}_{M,i}^*) - \nu_i c_l(\mathbf{p}_{M,i}^*)\}$   $\left[ H(\{\nu_{i,l}\}) = \sum_l r_l(\mathbf{p}_{M,i}^*) - \nu_{i,l} c_l(\mathbf{p}_{M,i}^*) \right]$ 
5:      $\nu_{i+1} = \min_l \frac{r_l(\mathbf{p}_{M,i}^*)}{c_l(\mathbf{p}_{M,i}^*)}$   $\left[ \nu_{i+1,l} = \frac{r_l(\mathbf{p}_{M,i}^*)}{c_l(\mathbf{p}_{M,i}^*)} \right]$ 
6:      $i = i + 1$ 
7:   end while
8:   return  $\mathbf{P}_M^* = \mathbf{p}_{M,i}^*$ 
9: end procedure

```

quasiconcave, and can be solved using a Dinkelbach's-like algorithm.

2) *Sum-EE formulation:* In this formulation, the total EE of IoT devices in the cell is used as an objective function, and thus such formulation tends to favor IoT devices with better coverage. More formally, we have

$$\underset{\mathbf{P}_M}{\text{maximize}} \quad \sum_{l=1}^N \bar{E}_l(\mathbf{P}_M), \quad (27)$$

subject to the same constraints as in (26).

The generalized Dinkelbach's algorithm for both SC-MD formulations is given in Algorithm 3, where the implementation of Sum-EE is given in brackets. We note for max-min, the algorithm converges linearly to the global optimal solution [42]. However, for the total EE formulation, the objective function is not necessarily quasiconcave, as the sum of quasiconcave functions does not preserve quasiconcavity. To this end, solving this problem globally, with limited complexity, remains an open problem, i.e., although Algorithm 3 has become popular to solve sum of ratios, it does not necessarily arrive at the global optimal solution, if it exists [43].

VI. SIMULATION RESULTS

In this section, we first validate the theoretical analysis and the stochastic optimization frameworks, focusing on SC-SD and SC-MD scenarios. Then, we consider larger networks, where we compare the proposed protocol with sharing-based and orthogonal-based protocols.

Unless otherwise stated, we use the simulation parameters given in Table I. In each spatial realization of the network, we generate the BSs, UEs, and IoT devices according to their distributions. Each drone then moves to their predetermined stop points. We then generate the

TABLE I: Main parameters

Description	Parameters
Path loss	$\alpha_G = 3.5$; $\alpha_A = 2.2$ [33]; $L_0 = -38\text{dB}$; $L_{\text{NLOS}} = -20\text{dB}$ [31]; $L_{\text{STR}} = -30\text{dB}$ [33]
BS parameters	$M_B = 32$; $U_B = 4$; transmission mode: multi-user zero-forcing
UE parameters	$P_U = 23\text{dBm}$; $\{\tau_{U,k}\}$ vary from -5 to 30dB
IoT device parameters	$P_M^{\max} = 23\text{dBm}$; $P_M^{\min} = 1\text{dBm}$; $\{\tau_{M,k}\}$ vary from -5 to 5dB ; $R = 50\text{m}$
Circuit power consumption	$P_{\text{CP}} = 20\text{dBm}$, $\eta = 0.3$

channel power gains according to their distributions and compute the large-scale fading for all links to compute their SINR, where a thermal noise power, with spectral density -174dBm/Hz , is considered at all receivers. Then the SE of UEs is computed via (4) and the EE IoT devices is computed via (5) for the different transmission protocols. We note that we use the actual load and LOS probability, instead of their mean, to compute the performance metrics.

A. Validation of the stochastic optimization frameworks

In this section, we focus on a single cell to validate the theoretical analysis. We further compare the EE performance of the SC-SD and SC-MD optimization frameworks with a scheme where the IoT device transmits at a maximum power, i.e., $P_M = 23\text{dBm}$ [5].

1) *Impact of IoT transmit power on the EE:* We consider two IoT categories: CAT-0 and NB-IoT. In the former, the IoT device shares the entire band with the UE, i.e., $W = 20\text{MHz}$ and $P_B = 46\text{dBm}$. In the latter, the IoT only shares a single resource block, i.e., $W = 180\text{KHz}$ and $P_B = 32\text{dBm}$ [44]. For interference protection, we assume $\epsilon = 0.5$ and $\rho_{\text{dB}} = -6\text{dB}$, i.e., the median ISR should not exceed -6dB . Fig. 4 shows the IoT EE for different transmit powers. We have the following remarks. First, the theoretical expression in (19) matches well with Monte Carlo simulations. Second, the EE is significantly improved using the proposed SC-SD framework compared to the max-power scheme, e.g., the EE in CAT-0 of the proposed SC-SD framework is 6x and 3x that of max-power for $h_D = 50\text{m}$ and $h_D = 300\text{m}$, respectively. This follows because the drone's location is optimized to minimize the 2D distance to the IoT device, requiring low transmit power for reliable coverage. Third, increasing the drone's height has two effects: an increase in the optimal transmit power and a decrease in the EE. These follow because as h_D increases, the received signal power decreases more rapidly than interference, degrading the coverage. Thus, the IoT device must transmit at higher power to combat the degradation,

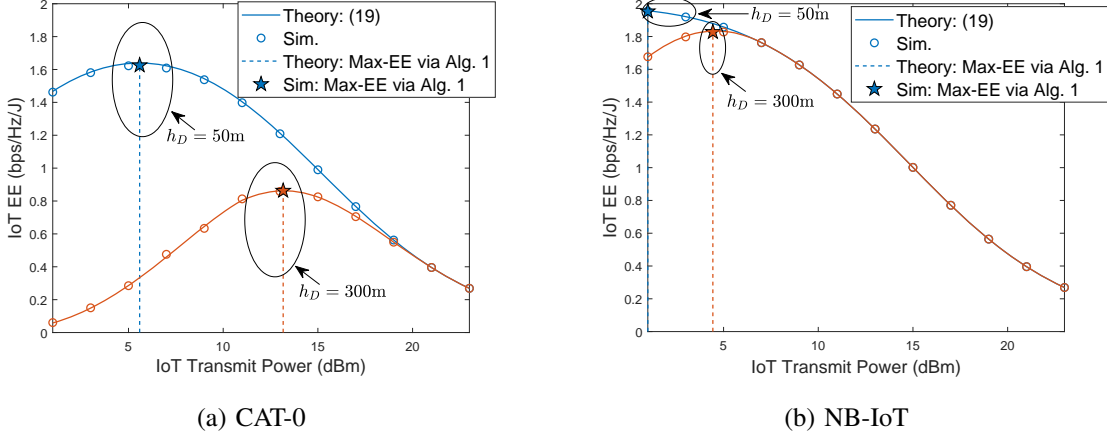


Fig. 4: The EE performance for different transmit powers.

decreasing its EE. Finally, the NB-IoT operation is more efficient than CAT-0 since in the former the IoT device shares a smaller number of carriers with the UE, reducing the interference.

2) *Impact of UAV-BS coordination:* We study the IoT EE performance when Algorithm 2 is used. We use the parameters of CAT-0, and consider two interference protection criteria: $\rho_{\text{dB}} = -6\text{dB}$ and $\rho_{\text{dB}} = -12\text{dB}$. Fig. 5a illustrates the convergence of the transmit powers of the BS and the IoT device, whereas Fig. 5b shows the evolution of the EE and the median ISR as the algorithm progresses. It is clear that the BS's transmit power decreases at first since the ISR constraint is satisfied with strict inequality. This allows the IoT device to further decrease its transmit power, which in return improves its EE, until the constraint is satisfied with equality. For instance, compared to the case of no-coordination, the EE improves roughly by 20% for $\rho_{\text{dB}} = -12\text{dB}$. We note that such gain comes at the expense of degrading the SINR of the UE.

3) *Validation of the SC-MD case:* Next, we study the EE performance in the presence of multiple drones in the same cell. We consider each drone to fly at one of the following altitudes: $h_D = [50, 100, 150, 200, 250]\text{m}$. In Fig. 6a, we show the total and the minimum EE of scheduled IoT devices per cell. We compare the max-power scheme to *Max-min* and *Sum-EE* schemes, where power allocation is done using Algorithm 3. We note that the EE is computed via Monte Carlo simulations. As expected, the *Sum-EE* formulation achieves the highest total EE in a cell, yet the *Max-min* formulation provides tangible improvements to the worst case scenario, e.g., the minimum EE is 2.7x and 1.7x the minimum EE under *Max-power* and *Sum-EE*, respectively. We further show the EE of IoT devices that belong to the different drones in Fig. 6b. It is observed that the *Max-min* solution aims to improve the EE of devices connected to the drone with the

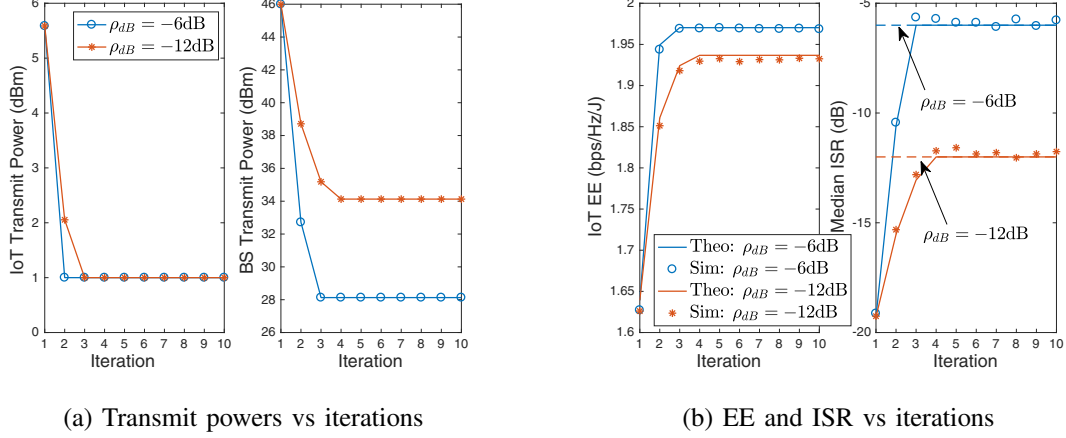


Fig. 5: EE and ISR performance under UAV-BS coordination.

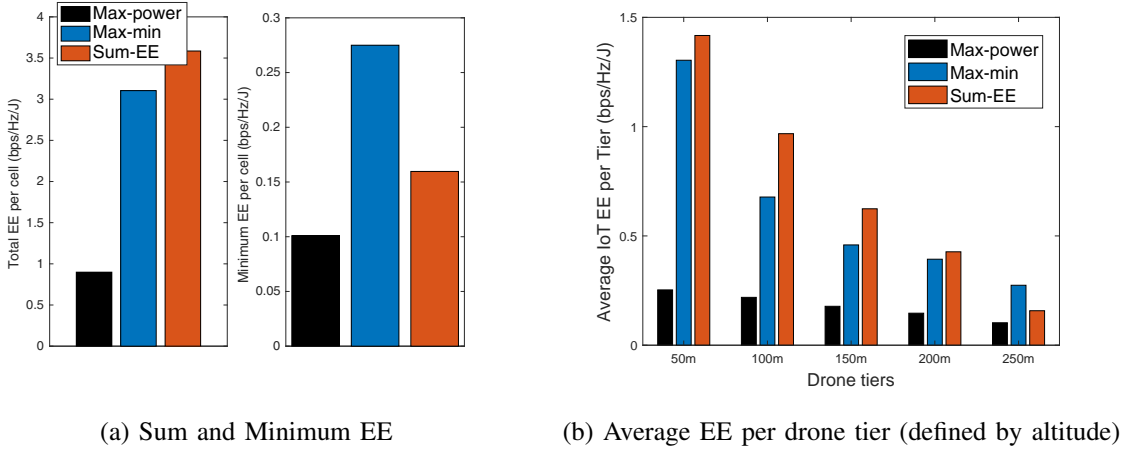


Fig. 6: EE performance for different schemes in the SC-MD case ($\rho_{dB} = -12dB$)

highest altitude as this tier achieves the lowest EE. In contrast, the *Sum-EE* formulation favors the drones with lower altitudes as they provide higher EE for IoT devices.

B. Performance comparison with existing protocols

In this section, we compare the performance of the proposed protocol with existing ones in large networks, and hence the results are obtained via Monte Carlo simulations. We also show the performance of UEs in the absence of IoT devices as a benchmark. For the proposed protocol, we consider three power allocation schemes: *Max-power*, *Max-EE* using the SC-SD framework (Algorithm 1), and *Max-EE* using exhaustive search, where we use extensive network simulations to search for the optimal power. We assume $\lambda_U = 50\lambda_B$ and $\lambda_{CI} = \lambda_D = 5\lambda_B$. Unless otherwise

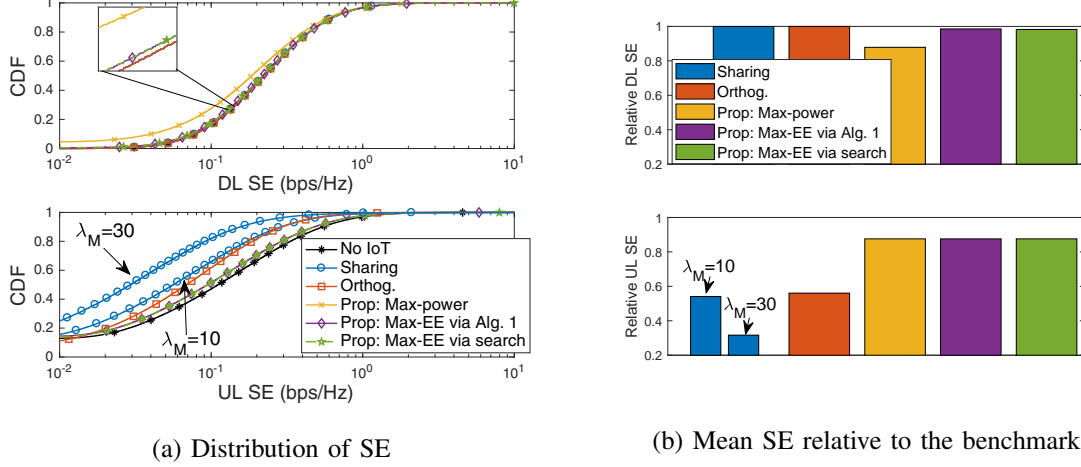


Fig. 7: UE DL and UL performance for the different protocols

stated, we consider $\delta = 1$, $W_U = 0.5W$, and $h_D = 50\text{m}$. We show the results assuming CAT-0 IoT devices (similar trends are observed for NB-IoT and hence omitted).

1) UE performance comparison: We first study the performance of the UE in the DL and the UL under different protocols. We note that both the orthogonal-based and the proposed protocols decouple the UE UL performance from the IoT density as in the former IoT devices use different frequency blocks, and in the latter IoT devices connect to drones instead of BSs. This is not the case for the sharing-based protocol, where we study the UE's performance for $\lambda_M = 10$ and $\lambda_M = 30$. Fig. 7a shows the distribution of the SE performance across all UEs and Fig. 7b shows the mean SE relative to the benchmark, i.e., the ratio of the mean SE under the given protocol to the mean SE in the absence of IoT devices. Since our model considers IoT devices to only operate in the UL, the DL SE of sharing-based and orthogonal-based protocols is the same as the benchmark. For the proposed protocol, it is shown that the DL degradation is minimal when the transmit power is optimized to limit the IoT interference. More importantly, the proposed protocols outperform existing ones in the UL, e.g., the relative mean UL SE of the proposed protocols is 1.6x and 2.8x the orthogonal-based and sharing-based ($\lambda_M = 30$) protocols, respectively. This follows due to the high congestion in the sharing-based protocol and the resource splitting in the orthogonal-based one.

2) IoT performance comparison: We then study the EE of the IoT under the different protocols. In Fig. 8a, the EE is shown for different densities of IoT devices. As expected, as the number of IoT devices increases, the EE decreases under all protocols. Yet, the proposed protocol

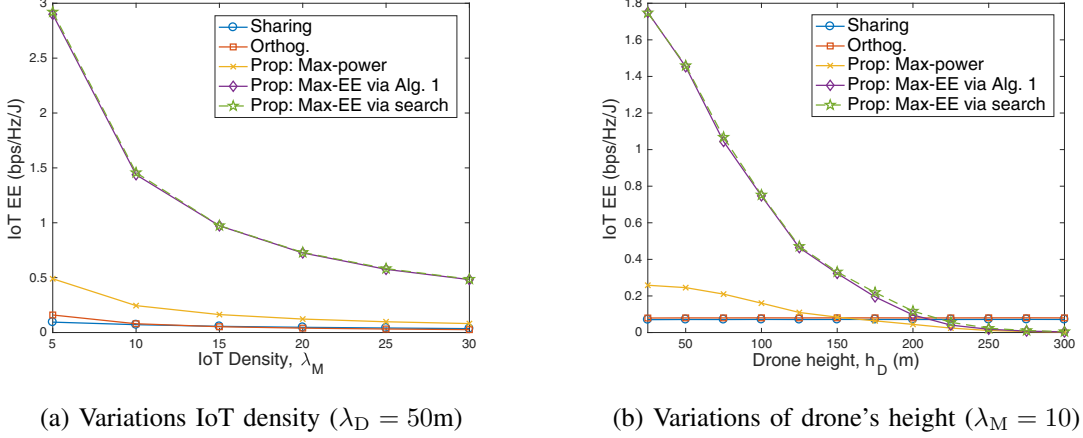


Fig. 8: IoT EE performance under different protocols

achieves the highest EE and scales better with λ_M compared to existing ones. It is also observed that it is beneficial to optimize the transmit power in tandem with the proposed protocol, i.e., the optimization framework ensures both lower interference on the UE (cf. Fig. 7) and higher IoT EE. In Fig. 8b, we study the EE for different drone's altitudes. We show the performance under the existing protocols, which do not depend on λ_D , for reference. It is observed that the proposed protocol is beneficial for lower altitudes. At very high altitudes, the received signal power is lower, and the LOS probability with interfering BSs, from different cells, increases. We note that in many regions, e.g., North America, Europe, China, etc., the maximum legal altitude for drones is roughly 120m (400ft), and thus the proposed solution is superior in practical scenarios.

3) *Impact of ACB and resource splitting:* Fig. 9 shows the IoT EE versus the UE SE in the UL under different ACB thresholds κ (Fig. 9a), and different frequency allocation ratios W_U (Fig. 9b). The performance of the proposed protocol, which does not depend on these parameters is also shown for reference. It can be seen that existing protocols have operating points with higher UE SE performance in comparison with proposed ones. However, high ACB threshold and frequency partitioning ratio are needed, and thus the IoT device will be limited with time and frequency resources, respectively. Finally, it is shown the SC-SD framework leads to a nearly identical performance to exhaustive search, yet the latter requires extensive simulations to solve.

VII. CONCLUSIONS

In this work, we have proposed a TDD protocol for a shared spectrum access between massive IoT and cellular UEs with UAVs acting as data aggregators. Using stochastic geometry, it

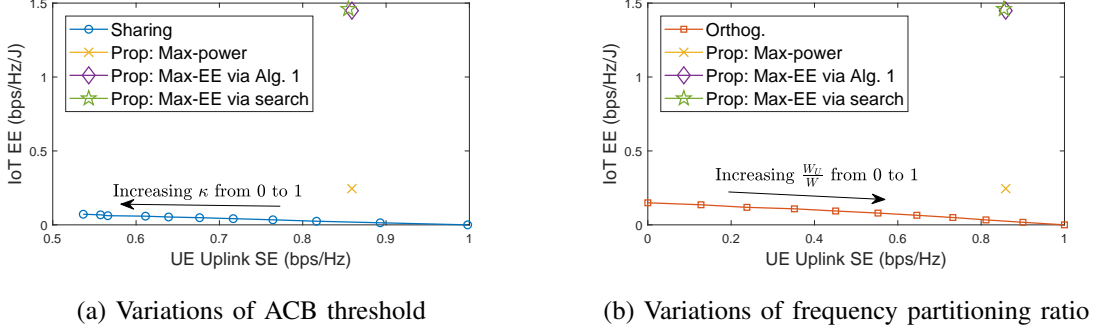


Fig. 9: IoT energy-efficiency vs. UE spectral efficiency ($\lambda_M = 10$ and $h_D = 50\text{m}$)

is shown that the protocol improves the average allocated resources of IoT devices and UEs compared to resource splitting and ACB, yet UEs experience additional interference from IoT devices. Thus, we have optimized the transmit power of the IoT device to maximize its energy-efficiency while constraining the interference on UEs. The analysis of the stochastic optimization framework is validated via simulations for the single-cell case. For larger networks, Monte Carlo simulations have shown that the proposed system significantly improves the EE with minimal degradation on the UE spectral-efficiency.

The key insights gleaned from this work are as follows. First, it is beneficial for drones to fly at lower altitudes as higher altitudes increase the LOS with interferers, forcing the IoT device to increase its transmit power to combat coverage degradation, which eventually affects its EE. In case drones, belonging to the same BS, fly at different altitudes, then maximizing the minimum EE and the total EE amount to prioritizing devices connected to drones at the highest and the lowest altitudes, respectively. Second, the extended coverage mode, where IoT devices transmit at maximum power, is not necessarily energy efficient as the gain in coverage does not outweigh the loss in power consumption. Finally, when the network is not interference-limited, we can improve the IoT EE by jointly coordinating the transmit powers of IoT devices and BSs.

APPENDIX

A. Proof of Theorem 1

Recall that the aggregate interference at the UE is given as

$$I_U = \underbrace{\sum_{y_b \in \Phi'_B} f_b y_b^{-\alpha_G}}_{I_{U,B}} + \underbrace{\sum_{z_m \in \Phi'_M} \frac{P_M}{P_B/U_B} f_m z_m^{-\alpha_G}}_{I_{U,M}}, \quad (28)$$

where we have normalized the interference by $L_0 P_B / U_B$. Using the Gil-Pelaez Inversion theorem [38] to evaluate the interference CDF, we get

$$F_{I_U} \left(\frac{g_B}{\tau x^{\alpha_G}} \right) = \frac{1}{2} - \frac{1}{\pi} \int_0^\infty \text{Im} \left\{ \varphi_{I_U}(x^{\alpha_G} t) e^{-jtg_B/\tau} \right\} dt, \quad (29)$$

where $\varphi_{I_U}(x^{\alpha_G} t) = \mathbb{E}_{I_U} [\exp(jtx^{\alpha_G} I_U)]$ is the characteristic function (CF), which is given as

$$\varphi_{I_U}(x^{\alpha_G} t) \stackrel{(a)}{=} \mathbb{E}_{I_{U,B}} \left[\exp \left(jtx^{\alpha_G} \sum_{y_b \in \Phi'_B} f_b y_b^{-\alpha_G} \right) \right] \mathbb{E}_{I_{U,M}} \left[\exp \left(jtx^{\alpha_G} \sum_{z_m \in \Phi'_M} \frac{P_M}{P_B/U_B} f_m z_m^{-\alpha_G} \right) \right], \quad (30)$$

where (a) follows since interfering BSs are independent from the interfering IoT devices.

Using the probability-generating functional of the HPPP process [29], it can be shown that $\varphi_{I_{U,B}}(x^{\alpha_G} t) = \exp(\pi \lambda_B x^2 (1 - \mathbb{E}_{f_b}[\Omega(f_b, \delta_G, t)]))$, where $\Omega(f_b, \delta_G, t) = {}_1F_1(-\delta_G; 1 - \delta_G; jt f_b)$, and ${}_1F_1(a; b; c)$ is the confluent hypergeometric function [45]. Similarly, we have

$$\begin{aligned} \varphi_{I_{U,M}}(x^{\alpha_G} t) &\stackrel{(a)}{=} \exp \left(-2\pi \lambda_D \int_0^\infty y \left(1 - \mathbb{E}_{f_m} \left[e^{jt \frac{U_B P_M f_m x^{\alpha_G}}{P_B y^{\alpha_G}}} \right] \right) dy \right) \\ &\stackrel{(b)}{=} \exp \left(-\delta_G \pi \lambda_D x^2 \int_0^\infty l^{-(1+\delta_G)} \left(1 - \frac{1}{1 - jtl \frac{P_M}{P_B/U_B}} \right) dl \right) \\ &= \exp \left(-\pi \lambda_D x^2 \hat{P}_{B,M}^{\delta_G} (-jt)^{\delta_G} \right), \end{aligned} \quad (31)$$

where (a) follows using the fact that the set of interfering IoT devices can be modeled as a set of Poisson interferers with density of λ_D as one IoT device is scheduled per drone per time-frequency slot, and (b) follows using the CF of f_m and then using the substitution $l = x^{\alpha_G} y^{-\alpha_G}$. Here, the integral lower limit is zero as the set of interfering IoT devices is independent of the UE's location, i.e., no protection zone is present unlike the case of interfering BSs which cannot be closer than the tagged BS. To summarize, we have $\varphi_{I_U}(x^{\alpha_G} t) = \exp \left(\pi \lambda_B x^2 \left(1 - \mathbb{E}_f[\Omega(f_b, \delta_G, t)] - (\lambda_D/\lambda_B) \hat{P}_{B,M}^{\delta_G} (-jt)^{\delta_G} \right) \right)$. Thus, the coverage becomes

$$\mathbb{C}_{U,DL}^P(\tau) = \frac{1}{2} - 2\lambda_B \int_0^\infty \frac{1}{t} \text{Im} \left\{ \varphi_g(-t/\tau) \Xi(t) \right\} dt, \quad (32)$$

where $\varphi_{g_B}(-t/\tau) = (1 + jt/\tau)^{-\Delta_B}$ is the CF of g_B and

$$\begin{aligned} \Xi(t) &= \int_0^\infty x e^{-\pi \lambda_B x^2 (\mathbb{E}_f[\Omega(f_b, \delta_G, t)] + (\lambda_D/\lambda_B) \hat{P}_{B,M}^{\delta_G} (-jt)^{\delta_G})} dx \\ &= \frac{(2\pi \lambda_B)^{-1}}{\mathbb{E}_f[\Omega(f_b, \delta_G, t)] + (\lambda_D/\lambda_B) \hat{P}_{B,M}^{\delta_G} (-jt)^{\delta_G}}. \end{aligned} \quad (33)$$

Plugging (33) in (32) and using $\mathbb{E}_f[\Omega(f_b, \delta_G, t)] = {}_2F_1(\Psi_G, U_B; 1 - \delta_G; jt)$, we arrive at (11).

B. Proof of Proposition 1

Let the IoT device be at a distance x_M from the drone. Then, the received signal power at the drone is given as

$$\begin{aligned}
\mathbb{P}(S_M \leq \tau) &= \mathbb{P}(P_M L_0 x_M^{-\alpha_A} L_0 ((1 - L_{\text{NLOS}}) \mathbb{P}_{\text{LOS}}(x_M, h_D) + L_{\text{NLOS}}) \leq \tau) \\
&\stackrel{(a)}{\approx} \mathbb{P}(P_M L_M x_M^{-\alpha_A} \leq \tau) \\
&= 1 - F_{x_M} \left(\left(\frac{P_M L_M}{\tau} \right)^{1/\alpha_A} \right) \\
&\stackrel{(b)}{=} \begin{cases} 1 - \frac{(P_M L_M / \tau)^{\delta_A} - h_D^2}{R^2}, & \frac{P_M L_M}{(R^2 + h_D^2)^{1/\delta_A}} \leq \tau \leq \frac{P_M L_M}{h_D^{1/\delta_A}} \\ 0, & \text{otherwise} \end{cases},
\end{aligned} \tag{34}$$

where (a) follows by using the mean LOS probability instead of the actual one, and (b) follows using the CDF of the distance between the typical IoT device and the drone $F_{x_M}(\cdot)$, which can be found using the fact that the IoT device is randomly distributed over an area of radius R centered around the 2D coordinates of the drone. Similarly, let r_B denote the distance between the tagged BS and the drone, then $\mathbb{P}(I_B \leq \tau) \approx \mathbb{P}(P_B L_B r_B^{-\alpha_A} \leq \tau) = 1 - F_{r_B} \left(\left(\frac{P_B L_B}{\tau} \right)^{1/\alpha_A} \right)$. Recall that the distance between a point in \mathbb{R}^2 and the nearest BS is distributed as $f_{y_B}(y) = 2\pi\lambda_B y \exp(-2\pi\lambda_B y^2)$ [36]. Thus, the distribution of $r_B = \sqrt{y_B^2 + h_D^2}$ can be found using a simple transformation, leading to $f_{r_B}(r) = \frac{2rf_{y_B}(\sqrt{r^2 - h_D^2})}{\sqrt{r^2 - h_D^2}}$. Thus, we can compute $F_{r_B}(r) = \int_{h_D}^{\infty} f_{r_B}(r) dr$ to arrive at (17).

C. Proof of Proposition 2

We first derive useful properties for $r(p)$. In particular, $r(p)$ is a non-negative sum of coverage probabilities, each is non-decreasing with the transmit power, and thus $r(p)$ is non-decreasing with p . Thus, the t -sublevel sets, i.e., $\mathcal{R}_{t,\text{sub}} = \{p | r(p) \leq t\}$, and the t -superlevel sets, i.e., $\mathcal{R}_{t,\text{sup}} = \{p | r(p) \geq t\}$, are convex, and hence $r(p)$ is quasilinear [41]. To show that $r(p)$ is S-shaped, we take the 2nd derivative with respect to p to get

$$\begin{aligned}
\frac{d^2 r(p)}{dp^2} &= \delta_A \pi \lambda_B \tilde{L}_M^2 (P_B L_B)^{\delta_A} \sum_{k=1}^{K_M} \frac{\mu_k e^{-\pi \lambda_B \left(\frac{p \tilde{L}_M - P_N}{\tau_{M,k} P_B L_B} \right)^{-\delta_A}}}{\tau_{M,k}^2 \left(\frac{p \tilde{L}_M}{\tau_{M,k}} - P_N \right)^{2(1+\delta_A)}} \times \left\{ \delta_A \pi \lambda_B (P_B L_B)^{\delta_A} \right. \\
&\quad \left. - (1 + \delta_A) \left(\frac{p \tilde{L}_M}{\tau_{M,k}} - P_N \right)^{\delta_A} \right\}.
\end{aligned} \tag{35}$$

Note that $\left(\frac{p\tilde{L}_M - P_N}{\tau_{M,k} P_B L_B}\right) \geq 0$ for any feasible $\tau_{M,k}$ and the derivative is non-increasing with p . Furthermore, there exists a point p^\bullet such that $\frac{d^2 r(p)}{dp^2} \geq 0$ for $p \leq p^\bullet$ and $\frac{d^2 r(p)}{dp^2} \leq 0$ for $p \geq p^\bullet$, and hence the function is S-shaped. To prove that $r(p)$ is concave when the condition in (23) holds, it is sufficient to show that the coverage $\mathbb{P}(\hat{\gamma}_M \geq \tau_k)$ is concave in p as $r(p)$ is a non-negative sum of the coverage probabilities. This can be shown by taking the second derivative of the coverage and showing that it is non-positive if and only if

$$\delta_A \pi \lambda_B (P_B L_B)^{\delta_A} - (1 + \delta_A) \left(\frac{p\tilde{L}_M - P_N}{\tau_k P_B L_B} \right)^{\delta_A} \leq 0, \quad (36)$$

which is satisfied when the condition in (23) holds.

To prove that the objective function in (22) is quasiconcave, then it is sufficient to prove that the superlevel sets $\mathcal{E}_{t,\text{sup}} = \{p | \frac{r(p)}{c(p)} \geq t\}$ are convex. Note since the objective is non-negative, then we only need to consider the case for $t \geq 0$ and prove that $\{p | r(p) - c(p)t \geq 0\}$ is convex. We consider two cases. First, for $p \geq p^\bullet$, $r(p)$ is concave, and thus for $p_1, p_2 \in \mathcal{E}_{t,\text{sup}}$ and $\beta \in [0, 1]$ we have

$$\begin{aligned} r(\beta p_1 + (1 - \beta)p_2) - c(\beta p_1 + (1 - \beta)p_2)t &\stackrel{(a)}{\geq} \beta r(p_1) + (1 - \beta)r(p_2) - c(\beta p_1 + (1 - \beta)p_2)t \\ &\stackrel{(b)}{=} \beta (r(p_1) - c(p_1)t) + (1 - \beta) (r(p_2) - c(p_2)t) \\ &\geq 0, \end{aligned} \quad (37)$$

where (a) follows because $r(p)$ is concave and (b) follows because $c(p)$ is affine, and thus, $\mathcal{E}_{t,\text{sup}}$ is convex. Second, for $p \leq p^\bullet$, $r(p)$ is convex. Taking the first derivative of $\bar{E}(p)$, we get

$$\frac{d\bar{E}(p)}{dp} = \frac{\eta^{-1}(pr'(p) - r(p)) + P_{\text{CP}}r'(p)}{c^2(p)}. \quad (38)$$

The second sum term $r'(p) \geq 0$ as $r(p)$ is a non-decreasing function in p . In addition, the first sum term $pr'(p) - r(p) \geq 0$ because $r(p)$ is convex, i.e., for any convex differentiable function $g(x)$ with $g(0) = 0$, we have $g(y) \geq g(x) + (y - x)g'(x)$ [41], and by setting $y = 0$ we get $xg'(x) \geq g(x)$. Thus, the derivative is non-negative, i.e., it is a non-decreasing function in $p \leq p^\bullet$, and hence the superlevel sets are convex, which completes the proof that the objective function is quasiconcave. To prove that the objective function is unimodal, note that $\bar{E}(0) = \bar{E}(\infty) = 0$, and since $\bar{E}(p)$ is quasiconcave, then it has to be unimodal.

REFERENCES

- [1] G. Hattab and D. Cabric, "Energy-efficient massive cellular IoT shared spectrum access via mobile data aggregators," in *IEEE 13th Int. Conf. Wireless and Mobile Computing(WiMob)*, Oct. 2017, pp. 1–6.
- [2] ITU-R, "IMT Vision – framework and overall objectives of the future development of IMT for 2020 and beyond," ITU-R, M. 2083-0, Sep. 2015.
- [3] McKinsey Global Institute, "The internet of things: Mapping the value beyond the hype," McKinsey&Company, Tech. Rep., Jun. 2015.
- [4] Z. Dawy, W. Saad, A. Ghosh *et al.*, "Toward massive machine type cellular communications," *IEEE Wireless Commun.*, vol. 24, no. 1, pp. 120–128, Feb. 2017.
- [5] 3GPP, "Cellular system support for ultra low complexity and low throughput internet of things, release 13," TS 45.820, 11 2015.
- [6] A. Rico-Alvarino, M. Vajapeyam, H. Xu *et al.*, "An overview of 3GPP enhancements on machine to machine communications," *IEEE Commun. Mag.*, vol. 54, no. 6, pp. 14–21, Jun. 2016.
- [7] Nokia, "LTE evolution for IoT connectivity," Tech. Rep., Jul. 2016.
- [8] A. Ali, W. Hamouda, and M. Uysal, "Next generation M2M cellular networks: challenges and practical considerations," *IEEE Commun. Mag.*, vol. 53, no. 9, pp. 18–24, Sep. 2015.
- [9] E. Soltanmohammadi, K. Ghavami, and M. Naraghi-Pour, "A survey of traffic issues in machine-to-machine communications over LTE," *IEEE Internet Things J.*, vol. 3, no. 6, pp. 865–884, Dec. 2016.
- [10] A. Laya, L. Alonso, and J. Alonso-Zarate, "Is the random access channel of LTE and LTE-A suitable for M2M communications? a survey of alternatives," *Commun. Surveys Tuts.*, vol. 16, no. 1, pp. 4–16, 2014.
- [11] P. K. Wali, A. A. N, and D. Das, "Optimal time-spatial randomization techniques for energy efficient IoT access in LTE-advanced," *IEEE Trans. Veh. Technol.*, vol. 66, no. 8, pp. 7346–7359, Aug. 2017.
- [12] Z. Feng, Z. Feng, and T. A. Gulliver, "Biologically inspired two-stage resource management for machine-type communications in cellular networks," *IEEE Trans. Wireless Commun.*, vol. 16, no. 9, pp. 5897–5910, Sep. 2017.
- [13] R. G. Cheng, J. Chen, D. W. Chen *et al.*, "Modeling and analysis of an extended access barring algorithm for machine-type communications in LTE-A networks," *IEEE Trans. Wireless Commun.*, vol. 14, no. 6, pp. 2956–2968, Jun. 2015.
- [14] Z. Wang and V. W. S. Wong, "Optimal access class barring for stationary machine type communication devices with timing advance information," *IEEE Trans. Wireless Commun.*, vol. 14, no. 10, pp. 5374–5387, Oct. 2015.
- [15] F. Morvari and A. Ghasemi, "Two-stage resource allocation for random access M2M communications in lte network," *IEEE Commun. Lett.*, vol. 20, no. 5, pp. 982–985, 2016.
- [16] 3GPP, "Separate backoff scheme for MTC," R2 103776, 2010.
- [17] O. Arouk, A. Ksentini, and T. Taleb, "Group paging-based energy saving for massive MTC accesses in LTE and beyond networks," *IEEE J. Sel. Areas Commun.*, vol. 34, no. 5, pp. 1086–1102, May 2016.
- [18] Y. Liang, X. Li, J. Zhang *et al.*, "Non-orthogonal random access for 5G networks," *IEEE Trans. Wireless Commun.*, vol. 16, no. 7, pp. 4817–4831, Jul. 2017.
- [19] W. Shin, M. Vaezi, B. Lee *et al.*, "Non-orthogonal multiple access in multi-cell networks: Theory, performance, and practical challenges," *IEEE Commun. Mag.*, vol. 55, no. 10, pp. 176–183, Oct. 2017.
- [20] N. Kouzayha, M. Jaber, and Z. Dawy, "M2M data aggregation over cellular networks: signaling-delay trade-offs," in *Proc. IEEE Globecom Workshops (GC Wkshps)*, Dec. 2014, pp. 1155–1160.
- [21] T. Kwon and J. M. Cioffi, "Random deployment of data collectors for serving randomly-located sensors," *IEEE Trans. Wireless Commun.*, vol. 12, no. 6, pp. 2556–2565, 6 2013.

- [22] D. Malak, H. S. Dhillon, and J. G. Andrews, "Optimizing data aggregation for uplink machine-to-machine communication networks," *IEEE Trans. Commun.*, vol. 64, no. 3, pp. 1274–1290, Mar. 2016.
- [23] U. Tefek and T. J. Lim, "Relaying and radio resource partitioning for machine-type communications in cellular networks," *IEEE Trans. Wireless Commun.*, vol. 16, no. 2, pp. 1344–1356, Feb. 2017.
- [24] J. Guo, S. Durrani, X. Zhou *et al.*, "Massive machine type communication with data aggregation and resource scheduling," *IEEE Trans. Commun.*, vol. 65, no. 9, pp. 4012–4026, Sep. 2017.
- [25] Y. Zeng, R. Zhang, and T. J. Lim, "Throughput maximization for UAV-enabled mobile relaying systems," *IEEE Trans. Commun.*, vol. 64, no. 12, pp. 4983–4996, Dec. 2016.
- [26] M. Mozaffari, W. Saad, M. Bennis *et al.*, "Mobile unmanned aerial vehicles (UAVs) for energy-efficient internet of things communications," *IEEE Trans. Wireless Commun.*, vol. 16, no. 11, pp. 7574–7589, Nov. 2017.
- [27] N. H. Motlagh, M. Bagaa, and T. Taleb, "UAV-based IoT platform: A crowd surveillance use case," *IEEE Commun. Mag.*, vol. 55, no. 2, pp. 128–134, Feb. 2017.
- [28] H. Menouar, I. Guvenc, K. Akkaya *et al.*, "UAV-enabled intelligent transportation systems for the smart city: Applications and challenges," *IEEE Commun. Mag.*, vol. 55, no. 3, pp. 22–28, Mar. 2017.
- [29] M. Haenggi, *Stochastic Geometry for Wireless Networks*. Cambridge University Press, 2012.
- [30] L. H. Afify, H. ElSawy, T. Y. Al-Naffouri *et al.*, "A unified stochastic geometry model for MIMO cellular networks with retransmissions," *IEEE Trans. Wireless Commun.*, vol. 15, no. 12, pp. 8595–8609, Dec. 2016.
- [31] M. Mozaffari, W. Saad, M. Bennis *et al.*, "Unmanned aerial vehicle with underlaid device-to-device communications: Performance and tradeoffs," *IEEE Trans. Wireless Commun.*, vol. 15, no. 6, pp. 3949–3963, Jun. 2016.
- [32] A. Al-Hourani, S. Kandeepan, and S. Lardner, "Optimal LAP altitude for maximum coverage," *IEEE Wireless Commun. Lett.*, vol. 3, no. 6, pp. 569–572, Dec. 2014.
- [33] 3GPP, "Study on enhanced LTE support for aerial vehicles," TR 36.777, Dec. 2017.
- [34] —, "Study on 3D channel model for LTE," TR 36.873, Sep. 2017.
- [35] W. Bao and B. Liang, "Rate maximization through structured spectrum allocation and user association in heterogeneous cellular networks," *IEEE Trans. Commun.*, vol. 63, no. 11, pp. 4510–4524, Nov. 2015.
- [36] Y. Lin, W. Bao, W. Yu *et al.*, "Optimizing user association and spectrum allocation in HetNets: A utility perspective," *IEEE J. Sel. Areas Commun.*, vol. 33, no. 6, pp. 1025–1039, Jun. 2015.
- [37] A. Zappone, L. Sanguinetti, G. Bacci *et al.*, "Energy-efficient power control: A look at 5G wireless technologies," *IEEE Trans. Signal Process.*, vol. 64, no. 7, pp. 1668–1683, Apr. 2016.
- [38] J. Gil-Pelaez, "Note on the inversion theorem," *Biometrika*, vol. 38, no. 3-4, Dec. 1951.
- [39] M. Haenggi, "The mean interference-to-signal ratio and its key role in cellular and amorphous networks," *IEEE Wireless Commun. Lett.*, vol. 3, no. 6, pp. 597–600, Dec. 2014.
- [40] H. Wei, N. Deng, W. Zhou *et al.*, "Approximate SIR analysis in general heterogeneous cellular networks," *IEEE Trans. Commun.*, vol. 64, no. 3, pp. 1259–1273, Mar. 2016.
- [41] S. Boyd and L. Vandenberghe, *Convex Optimization*. Cambridge University Press, 2004.
- [42] J.-P. Crouzeix and J. A. Ferland, "Algorithms for generalized fractional programming," *Mathematical Programming*, vol. 52, no. 1, pp. 191–207, 1991.
- [43] S. Schaible and J. Shi, "Fractional programming: the sum-of-ratios case," *Optimization Methods and Software*, vol. 18, no. 2, pp. 219–229, 2003.
- [44] Industry White Paper, "Coverage analysis of LTE-M category-M1," Tech. Rep., 2017.
- [45] A. Jeffrey and D. Zwillinger, *Table of Integrals, Series, and Products*. Elsevier LTD, Oxford, 2014.